BIOMASS ESTIMATION USING DIGITAL PHOTOGRAMMETRIC CAMERAS

F. Alvarez [a, *], T. Catanzarite [b], J. Castellanos [c], V. Blanco Medina [d]

[a] Universidad de León. Campus de Ponferrada, s/n 24400. Ponferrada (Leon, Spain). flor.alvarez@unileon.es
[b] Universidade de Vigo. Campus Universitario, s/n 36310 Vigo (Pontevedra, Spain). tainyct@gmail.com
[c] Wideworld Geographic Services. 48902 Barakaldo (Bizcaia, Spain) javier.castellanos@wideworld.es
[d] ITACYL. Junta de Castilla y Leon. Finca Zamadueñas. 47071 (Valladolid, Spain) blamedvi@itacyl.es

KEY WORDS: camera, radiometric, calibration, thematic, biomass, forestry, National Plan of Aerial Orthophotography (PNOA)

ABSTRACT:

Estimating and modelling biomass can be helpful for biomass management. It is also interesting to calculate the amount of biomass in a certain area for carbon implications, as indicated by the Kyoto protocol. In the past remote sensing techniques have been able to estimate biomass by using reflectance in the both the red and the near infrared wavelengths. Nowadays the sensors in the digital photogrammetric cameras gather information not only in the visible wavelengths but also in the near infrared wavelengths, which provides the possibility of using digital photogrammetric data for environmental studies. The National Plan of Aerial Orthophotography (PNOA) updates the photogrammetric information (e.g. orthophotographs) in Spain every two years, but so far none of the data derived from the photogrammetric flights is used to extract thematic or biophysical information. Therefore it would be interesting to explore the possibility of establishing a relationship between the biomass and the radiometric information captured by the digital photogrammetric cameras, as an added value to the PNOA deliverables. The aim of this research is determining the suitability of the Ultracam X and Ultracam Xp for biomass estimation in grasslands.
There are two different study areas in this research. Field A is located in a grassland area in Barakaldo (Bizcaia, Spain). Field B is located in a grassland area in Cogollos (Burgos, Spain). The aerial photograph of Field A was captured by a digital photogrammetric camera Ultracam X with a Ground Sampling Distance (GSD) of 7 cm, while Field B was flown as part of the PNOA with a digital photogrammetric camera Ultracam Xp and a GSD of 25 cm. The images were calibrated to at-surface reflectance using ten portable reflectance targets with nominal reflectance values of 0%, 25%, 50%, 75% and 100%. An empirical line calibration was performed using the reflectance values for the targets and the corresponding Digital Numbers (DNs) in the images.
20 sample plots were placed in each study area to estimate their biomass and to be characterized radiometrically. Each of the 1 m x 1 m sample plots were radiometrically characterized by using the average radiance/reflectance values obtained for the sub-plots (0.50 x 0.50 m) using an ASD Fieldspec®3 spectrometer. The dried biomass weight was calculated to characterize each one of the plots to be used as a surrogate for the aboveground dry biomass.
The data analyses were conducted in two ways: (i) the relationships between the radiometric values registered by the spectrometer for each sub-plot and the biomass estimation were studied and (ii) the relationships between the radiometric data gathered/derived for each sub-plot/plot by the aerial camera and the biomass estimation were investigated. The data was then analyzed by study area and the results of the study areas were compared, in order to study the influence of GSD.

1. INTRODUCTION

The possibility of estimating the vegetation biomass and its modelling can aid in crop management regarding the estimation of the yield and the management of its residuals. It is also crucial to know the amount of biomass in a certain area due to its direct relationship with carbon and the holistic study of the agri-forest systems as carbon sinks. The Kyoto protocol requires the evaluation of the productivity of forested areas to determine carbon stocks. Measuring biomass directly is a destructive and expensive procedure, so forest researchers and managers are looking for non destructive and repeatable methods to monitor biomass. Remote sensing techniques meet the two previous requirements, and in addition, they allow both spatial and temporal analysis.
The reflectance in the red and the near infrared (NIR) bands have been used in several studies to analyse the relationship between reflectance and vegetation (Jensen, 2005). Moreover, the vegetation indices derived from the red and the near infrared (NIR) bands (e.g. simple ratio, normalized vegetation index) have been used to estimate biomass (e.g. Rouse et al., 1974 (in: Jensen, 2005); Nitch et al., 1991, Cho et al., 2007)
Nevertheless, several studies have shown that the computation of NDVI with wide spectral bands can be unstable and inadequate to estimate biomass, due to variations in the colour of the soil, the canopy structure and/or atmospheric conditions. Moreover, the NDVI that is calculated using this data can reach an asymptotic value once a certain biomass value is achieved (Gao et al, 2000).
Nowadays the sensors in the digital photogrammetric cameras gather information not only in the visible wavelengths but also in near infrared wavelengths, which provides the possibility of using digital photogrammetric data for environmental studies. PNOA updates the photogrammetric information (e.g. orthophotographs) in Spain every two years, but so far none of the data derived from the photogrammetric flights is used to extract thematic or biophysical information; therefore, it would be interesting to explore the possibility of establishing a relationship between the biomass and the radiometric information captured by the digital photogrammetric cameras, as an added value to the PNOA deliverables. The aim of this

* Corresponding author.

research is determining the suitability of the Ultracam X and Ultracam Xp for biomass estimation in grasslands.

2. MATERIAL

2.1 Imagery

Two different data sets of multispectral images were used to conduct this research. Set A consisted of three images captured by the digital photogrammetric camera Ultracam X with a GSD of 7 cm in Barakaldo (Bizcaia, Spain) on the 12th July 2009. The images were taken so that the geometric centre of each image was as close as possible to reflectance targets that were placed in the field. These images were originally processed to level 2 (according to the camera's technical specifications). Set B consisted of two images gathered by the digital photogrammetric camera Ultracam Xp with a GSD of 25 cm in Cogollos (Burgos, Spain) on the 10th July 2009 as part of PNOA. The images in set B were already processed to level 3 (according to the camera's technical specifications), since it is the default processing level for all of the images acquired for PNOA in 2009. More details about the imagery characteristics can be found in a previous journal article (Alvarez et al., 2010).

2.2 Reflectance targets

10 portable reflectance targets were used for the calibration process. The 1m x 1 m targets were made of Alucobond® and coated with vinyl. The selected reflectance values were 100% (BL), 75% (GR25), 50% (GR50), 25% (GR75) and 0% (NG). Also two targets were manufactured for each reflectance value. According to Baugh and Groeneveld (2008) the ground target surfaces to be used in an empirical line calibration are required to be: homogeneous, at least 5 x 5 pixels in size, of contrasting albedo, and ideally spectrally featureless. Those characteristics are met by the reflectance targets used in this study regarding Set A, but not for set B, since in set B the targets are smaller than the recommended size for images with a GSD of 25 cm.
As shown in previous work (Alvarez et al., 2010), the nominal reflectance values were different from the reflectance values measured with the ASD Fieldspec®3 spectrometer immediately before the flight; therefore, the values obtained with the spectrometer were used as reference. Ten readings (i.e. each of the measurements gathered by the instrument) were collected per panel by the spectrometer. All of the ten readings were within a spectral range from 350 nm to 2500 nm. The readings were checked and the outliers filtered out in order to assign the mean values to the target. The targets were placed in the corresponding calibration field before the flights, and the GPS coordinates of the exterior corners were measured using a double frequency GPS Trimble 5700. The data gathered was post-processed using reference stations in order to refer the coordinates to ETRS 89 and locate the targets accurately. These points were then used to check the accuracy of the overlap between the processed imagery and the locations gathered with the GPS.

2.3 Biomass data

20 sample plots were placed in each study area to estimate their biomass and to be characterized radiometrically. Each 1 m x 1 m plot was located on a 2 m x 2 m homogeneous area covered by species of the *Gramineae* family. Each plot was then divided into 4 sub-plots (0.50 x 0.50 m). The plot locations were determined using a 24-channel dual-frequency RTK GPS receiver Trimble 5700, with a precision of 5 mm in static surveying mode. The GPS data was post-processed using reference stations in order to refer the coordinates to ETRS 89. In Field B both the radiance and reflectance were measured for each sub-plot with the spectrometer Fieldspec®3 immediately after the aerial image was captured, while in Field A only digital numbers were registered. Ten radiometric measurements were gathered for each sub-plot.

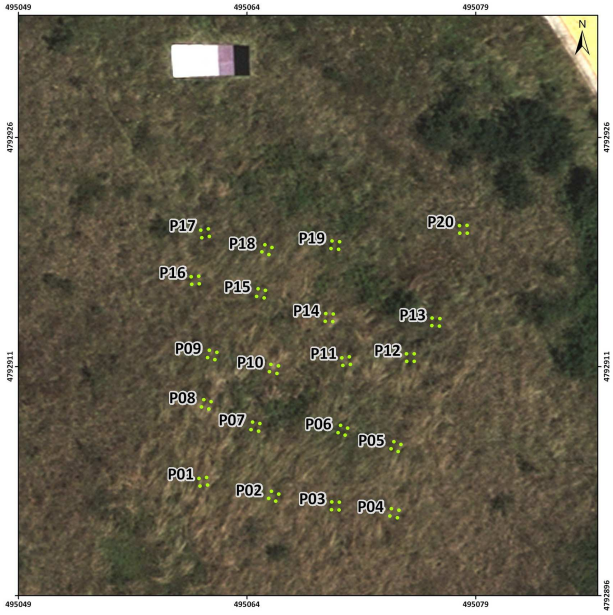

Figure 1. Location of the biomass plots (Pi), sub-plots (in green) and the reflectance targets in the data set A (Barakaldo).

All of the biomass in each sub-plot was harvested and weighed in the field using a portable scale. 10% of the biomass of each NW subplot was stored and kept as a representative sample to determine the plot biomass in the laboratory. The sample was weighed in the laboratory using a precision scale before drying it in an oven. The sample was weighed again using the precision scale after the sample was dried in the oven for 24, 36, and 48 hours at 65ºC, in order to obtain the dried biomass weight at 24 h, 36 h and 48 h. The dried biomass weight was used as surrogate for the aboveground dry biomass in each plot.

3. METHODS

3.1 Imagery pre-processing: geometric and radiometric correction

Images from both set A and set B were orthorectified using the Integrated Sensor Orientation (ISO) technique. The DNs in each one of the spectral bands were resampled using the nearest neighbour method, so that the original DNs were not modified. Three independent orthophotos were obtained for Barakaldo (7016, 7017, 7018), while for Cogollos only one orthophoto was generated. More details about the image processing can be found in Alvarez et al. (2010).
The main goal of the absolute radiometric correction was to calculate scaled surface reflectance values from the digital brightness values which were recorded by the aerial sensor. The empirical line calibration (ELC) was used for the atmospheric correction of remotely sensed data from at-sensor radiance or digital numbers to at-surface reflectance, as a first step to extract thematic (e.g. biophysical) data. This absolute radiometric correction relates the digital values and the surface reflectance values of some of the targets with different albedos which were located in the image. The linear relationship

between reflectance and the DNs for the dark (0% and 25% nominal reflectance) and the bright (75% and 100% nominal reflectance) targets were explored for each band in each orthophoto, in order to obtain a linear equation with a gain and an offset for each of the bands (Equation 1). The reflectance values for the BL_2 target were excluded for set B, since the BL_2 target was an outlier (its reflectance was smaller than the reflectance of all the other targets except for the black ones).

$$BV_k = \rho_\lambda A_k + B_k \quad (1)$$

Where: BV_k is the digital output value for a pixel in band k, ρ_λ is the scaled surface reflectance of the materials within the remote sensor Instantaneous Field Of Vision (IFOV) at a specific wavelength (λ), A_k is the "gain" and B_k "the offset" (Jensen, 2005).

The linear relationship was evaluated using the adjusted coefficient of determination r^2 (with a level of significance of 5% ($\alpha = 0.05$) for the model) and the standard error of the estimate (SEE). The adjusted r^2, unlike the r^2, takes into account the number of predictors and the number of observations. The SEE is the standard deviation of the error term, and is the square root of the mean square error. The linear regression assumptions regarding, linearity of the relationship between dependent and independent variables, independence of the errors, homoscedasticity of the errors, and normality of the error distribution, were tested by the analysis of the residuals.

After the gain and offset values were obtained they were applied to the corresponding orthophoto on a band by band basis, removing the atmospheric attenuation, and obtaining an at-surface reflectance image.

3.2 Biomass data processing

The biomass data was split into radiometric data and physical data, in order to characterize the biomass regarding both aspects.

The radiometric data gathered with the spectrometer for each sub-plot in set B was explored and the maximum and the minimum reflectance curves for each sub-plot where filtered out. The curve resulting from the median values of the remaining curves was then calculated. The spectral signature gathered for each sub-plot was reclassified, so that each wavelength was assigned to the corresponding Ultracam multispectral band. Therefore the wavelengths between 400-600 nm were labelled as blue band (B), 480-600 nm as green band (G), 580-720 nm as red band (R), and 620-1000 nm as infrared band (IR). These threshold values were chosen because they are the minimum and maximum wavelengths for each Ultracam band, although it cannot be assumed that the spectral sensitivity in these bands is constant between the maximum and minimum values.

In order to obtain representative reflectance values for each plot (Pi), the reclassified reflectance values for B, G, R and NIR for each corresponding set of sub-plots (Pi_j) were analyzed. The sub-plot reflectance distributions were compared in pairs (e.g. to obtain P1 values P1_1 and P1_2, P1_1 and P1_3, P1_1 and P1_4, P1_2 and P1_3, P1_2 and P1_4, and P1_3 and P1_4) to detect which sub-plots are more similar and therefore more suitable to be used to estimate the reflectance for the whole plot. Thus, the non-parametric Mann–Whitney U test for independent samples was conducted to calculate the reflectance values in bands B, G, R and NIR at a significance level of 5% ($\alpha = 0.05$). The plot reflectance was then calculated using the average reflectance of sub-plots that were not significantly different.

The dried weight biomass values (measured after drying in the oven for 24, 36 and 48 hours) were converted to g/m^2 units and therefore could be correlated to the plot. The biomass values could then be converted to carbon stocks using a conversion factor (carbon fraction of biomass). This was not available for the site species composition, nevertheless, the relationship is linear so the dried biomass can be used as a surrogate for carbon in relative terms.

3.3 Biomass estimation from remotely sensed data

The at-surface reflectance images for set A (3 orthophotos) and set B (1 orthophoto) were obtained using the empirical line calibration described in section 3.1. The reflectance values for these four images were gathered for the four spectral bands (B, G, R, NIR). Since the objective was to find a relationship between the biomass values and the spectral information, two vegetation indices were derived from the spectral data: the Simple Ratio (SR) and the Normalized Difference Vegetation Index (NDVI). The SR is a near infrared to red reflectance index described in Birth and McVey (1968) (Equation 2). The NDVI (Rouse et al., 1974) was calculated as shown in Equation 3.

$$SR = \frac{NIR}{red} \quad (2)$$

$$NDVI = \frac{NIR - red}{NIR + red} \quad (3)$$

Where: *NIR* and *red* are the reflectance values for the NIR and Red bands respectively.

Therefore each orthophoto had four reflectance bands (B, G, R, NIR) and two extra bands with the two vegetation indices. The values of the six bands were extracted individually for each of the pixels defining each sub-plot. The pixel values were explored in order to detect outliers. The reflectance and index values assigned to each biomass plot were computed as the mean value and median value of the sub-plot values. The Spearman's rank correlation coefficient (Spearman's rho) at significance level of 5% ($\alpha = 0.05$) was calculated to determine whether a correlation between the biomass (dried in the stove for 24, 36 or 48 hours) and the reflectance and/or vegetation indices existed. The significant relationships were modelled as a linear regressions, and evaluated using the adjusted coefficient of determination r^2 (with a level of significance of 5% ($\alpha = 0.05$) for the model), and the standard error of the estimate (SEE). The linear regression assumptions regarding, linearity of the relationship between dependent and independent variables, independence of the errors, homoscedasticity of the errors, and normality of the error distribution, were tested by the analysis of the residuals. The potential and logarithmic models were also tested.

The relationship between the dried biomass and reflectance was also explored using the spectral data gathered with the spectrometrer Fieldspec®3 in Cogollos. Moreover, the NDVI and the SSR were calculated using the reflectance values of the red and NIR bands. In order to test the existence of a linear relationship, the Spearman's rank correlation coefficient (Spearman's rho) at significance level of 5% ($\alpha = 0.05$) was calculated between the dried biomass weight per plot and: (i) the average reflectance values and (ii) the vegetation indices. This non-parametric test is a measure of statistical dependence which does not require a bivariate normal distribution for the data and therefore is more robust then the Pearson correlation coefficient. A stepwise linear regression analysis was also

conducted, including all the reflectance bands and vegetation indices as potential predictors and the dried biomass weight as dependent variable. The relationships were evaluated using the coefficient of determination r^2 and standard error of the estimate (SEE).

4. RESULTS AND DISCUSSION

4.1 Radiometric correction (Empirical line calibration)

Table 1 shows the summary of the linear regression model between the DNs and the reflectance values, per band and by orthophoto. The initial approach (excluding just the 50% reflectance targets) provided a high adjusted r^2 for set A (7016, 7017, 7018) for all bands except for the NIR band. Therefore a new regression was performed using only the 0%, 25% and 100% reflectance targets (6 targets in total). The adjusted r^2 for set A improved and was greater than 0.98. There were no significant differences ($\alpha = 0.05$) among the orthophotos for the adjusted r^2. The results for data set B (Cog) showed low values for the adjusted r^2 for the visible bands (less than 0.80) when using 5 targets. Therefore a regression with 5 targets (excluding the 50% and 75% reflectance targets) was conducted. The adjusted r^2 values that were obtained were greater than 0.85 for the B, G and R bands. For dataset B the ELC was applied to the orthophoto using both models (5 and 7 targets).

		Blue		Green		Red		NIR	
Ortho	N	A.R^2	SEE	A. R^2	SEE	A. R^2	SEE	A. R^2	SEE
7016	8	.963	1.15	.980	.84	.982	.821	.542	4.26
7017	8	.968	1.08	.982	.79	.987	.712	.563	4.16
7018	8	.968	1.10	.982	.81	.987	.726	.622	4.07
7016	6	.996	.38	.990	.57	.997	.345	.982	.83
7017	6	.997	.30	.990	.58	.998	.283	.982	.84
7018	6	.998	.29	.989	.61	.997	.358	.997	.40
Cog	7	.779	.14	.811	.13	.799	.122	.918	.09
Cog	5	.854	.12	.863	.12	.878	.107	.922	.10

Table 1. Summary of the linear model for the ELC. Ortho: Orthophoto (Cog: Cogollos), N: number of reflectance targets used in the regression, A.R^2: adjusted R^2, SEE: Standard Error of the Estimate.

The regression models, and therefore the "gain" and "offset" values obtained for each band were significantly different ($\alpha = 0.05$) in each of the three orthophotos in dataset A. The significance of the t value indicated that the offset and gain were significantly different from 0 for all of the orthophotos in dataset A using an 8 target model for calculating regression. The results of using the 6 target model for calculating regression showed that the offset values were not significantly different from 0 for the B, G and R bands for orthophoto 7018. This result indicated that the reflectance would be directly proportional to the DNs, which does not fit the theoretical model and would recommend the rejection of the 6 target model for visible bands in this orthophoto. Nevertheless, the model was adequate for the NIR band in all cases. Therefore the models using 8 targets were used to correct the B, G, R bands and the models using 6 targets were used to correct the NIR bands for all the three orthophotos in set A. Table 2 shows the regression model for orthophoto 7018 using 8 targets for B, G, and R bands, and 6 targets for the NIR band. The coefficient corresponding to the gain and offset (A and B in equation 1), the standard errors associated with the coefficients, and their 95% confidence interval limits are also displayed in the table.

Regression model				95% Confidence interval limit	
Band		Coef.	S. Error	Lower	Higher
BLUE	offset	-1.287	.103	-1.490	-1.084
	gain	.099	.001	.097	.101
GREEN	offset	-.546	.072	-.688	-.404
	gain	.084	.001	.083	.085
RED	offset	-.740	.065	-.868	-.612
	gain	.101	.001	.099	.102
NIR	offset	-2.796	.056	-2.907	-2.685
	gain	.072	.000	.071	.072

Table 2. Linear model for the ELC for the orthophoto 7018. Coef.: coefficient, S. Error: standard error.

Table 2 summarizes the regression model for the orthophoto from Cogollos using 5 targets. The results showed that the offset values were not significantly different from 0 for the B, G and R bands. This result indicates that the DNs and the reflectance would be directly proportional, which does not fit the theoretical model and would suggest the rejection of the 5 target model and the use of a 7 target model.

Regression model				95% Confidence interval limit	
Band		Coef.	S. Error	Lower	Higher
BLUE	offset	-.065*	.035	-.135	.005
	gain	.003	.000	.002	.003
GREEN	offset	-.021*	.031	-.084	.042
	gain	.002	.000	.002	.003
RED	offset	-.019*	.028	-.076	.039
	gain	.002	.000	.002	.003
NIR	offset	-.348	.040	-.429	-.267
	gain	.004	.000	.004	.005

Table 3. Linear model for the ELC for Cogollos using 5 targets. Coef.: coefficient, S. Error: standard error. *not significantly different from 0 at a significance level of 5%.

4.2 Biomass estimation from remotely sensed data

Table 4 shows that none of the Spearman's rank correlation coefficients are significant in the analysis of the orthophoto for Cogollos. However, most of the coefficients are significant for the orthophotos from set A, and they were not significantly different regarding the biomass variable (24 h, 36 h or 48 h) considered for the correlation with the reflectance or the vegetation index values. The results achieved for orthophotos 7018 and 7017 were significantly better than the results obtained for orthophoto 7016. The biomass results were best correlated with the vegetation indices (SR and NDVI), followed by the blue band and then the red band. Four plots in data set A were identified as outliers after an exploratory analysis and were filtered out before the modelling was conducted.

		Dried biomass weight				Dried biomass weight		
Ortho	Band	B24	B36	B48	Band	B24	B36	B48
7016	B	.56*	.56*	.56*	NIR	.21	.21	.21
7017	B	**.72***	**.72***	**.72***	NIR	.23	.23	.23
7018	B	**.75***	**.75***	**.75***	NIR	.39	.39	.39
7016	G	.57*	.57*	.57*	SR	-.41	-.41	-.41
7017	G	.63*	.63*	.63*	SR	**-.70***	**-.70***	**-.70***
7018	G	**.71***	**.71***	**.71***	SR	**-.78***	**-.78***	**-.78***

7016	R	.45	.45	.45	NDVI	-.40	-.40	-.40
7017	R	.54*	.54*	.54*	NDVI	**-.60***	**-.60***	**-.60***
7018	R	**.75***	**.75***	**.75***	NDVI	**-.77***	**-.77***	**-.77***
Cog	B	.25	.18	.25	NIR	.12	.06	.12
Cog	G	.19	.12	.12	SR	-.23	-.19	-.23
Cog	R	.18	.13	.18	NDVI	-.23	-.19	-.23

Table 4. Spearman's rho correlation coefficient between the reflectance and the dried biomass weight (24 h, 36 h or 48 h) per band (B, G, R, NIR) and orthophoto. *correlation significant at the significance level of 5%.

Table 5 shows that the linear models adjusted by means of a regression for the dried biomass weight (48 h) and the spectral band and indices. The results for set B (Cogollos) are not shown because in all of the cases the adjusted r^2 was smaller than 0.1.

These results might be due to inaccuracies derived from the calibration process using the ELC method, positional inaccuracies when extracting the spectral information from the image, or because the GSD was too large (compared to the plot size) to gather information which were homogenous enough to be used in the analysis. The best results were obtained for the orthophoto 7018, as expected, after the previous correlation analysis.

	Ortho 7016		Ortho 7017		Ortho 7018	
BAND	A.R^2	SEE	A. R^2	SEE	A. R^2	SEE
Blue	.351	245.68	.469	222.32	.532	209.42
Green	.211	270.97	.371	241.91	.464	223.24
Red	.118	286.41	.350	245.94	.534	208.30
NIR	-.02	308.03	-.01	307.49	.071	294.01
SR	.151	280.99	.352	245.47	.642	182.41
NDVI	.135	283.67	.430	230.24	.606	191.49

Table 5. Summary of the linear model for biomass estimation. Ortho: Orthophoto, A.R^2: adjusted R^2, SEE: Standard Error of the Estimate.

The adjusted models for the spectral indices and dried biomass weight (48 h) (g/m^2) are shown in Table 6. Both the gain and offset were significantly different from 0 at a significance level of 5% in the models using SR and NDVI. However, using the red reflectance the offset for the model was not significantly different from 0, so it should therefore be removed from the model. The gain* shows the coefficient once the offset was removed from the model. The r^2 of this modified model (adjusted $r^2 = 0.90$) cannot be compared to the previous ones, because there is no intercept in the modified equation.

Regression model for Biomass (48h)				95% Confidence interval limit	
Variable		Coef.	S. Error	Lower	Higher
Red	offset	-124.55*	177.06	-504.32	255.21
	gain	3449.32	809.40	1713.31	5185.33
	gain*	2905.13	234.01	2406.35	3403.92
SR	offset	1783.01	229.03	1291.7	2274.2
	gain	-17.83	3.37	-25.0	-10.5
NDVI	offset	18882.22	3728.39	10885.6	26878.8
	gain	-19148.69	3904.06	-27522.0	-10775.3

Table 6. Linear model to estimate dried biomass weight (g/m^2) for orthophoto 7018. Coef.: coefficient, S. Error: standard error.

Figure 2 shows the regression lines corresponding to the models (which are shown in Table 6). A positive correlation between the reflectance and the dried biomass weight was expected (like all positive correlations with the visible bands), so using the red reflectance, as the model showed, is adequate according to the theoretical biophysical model. Considering that the relationship with the biomass should be saturated for high values of reflectance, the logarithmic model was adjusted, obtaining a better r^2 coefficient of determination.

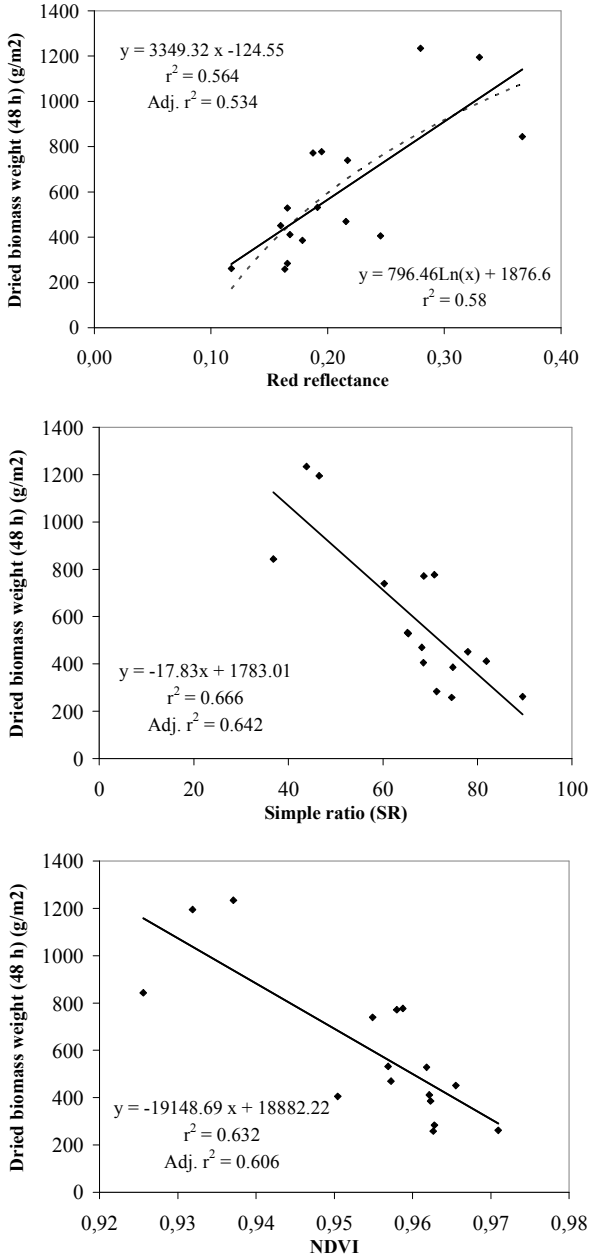

Figure 2. Regression line for dried biomass weight (48 h) and the red reflectance, the SR, and the NDVI for orthophoto 7018 (from the top to the bottom). Linear models are shown with a continuous line, while the logarithmic model is shown with a discontinuous line.

The good performance of the red reflectance can be related to the wavelengths gathered by the Ultracam red band (580-720 nm), which means that the reflectance from the *red edge* region (680 nm to 730 nm) is captured. The *red edge* is the region of rapid change in reflectance of chlorophyll in the near infrared

range, which is very useful to monitor vegetation characteristics (Jensen, 2005).

The models which involve the vegetation indices show a negative correlation, i.e. increasing values in the NDVI, which means decreasing values in the biomass output. NDVI and SR are related to photosynthetic activity, and the relationship between biomass and these indices needs to be established at different stages in plant development. Barrachina et al. (2009) found a negative relationship between the dried biomass weight and the NDVI for grassland in the Pyrenees for different months during the summer. The relationship was more negative for the month of July than the month of August. Therefore the model obtained using the vegetation indices needs to be adjusted for other phenological states. Moreover the NDVI values vary from 0.92 to 0.98, which limits the applicability of this model to grasslands in similar conditions. Therefore it is recommended to complete the research by increasing the number of sample plots with more variability in the NDVI values. The logarithmic and exponential models were also adjusted for the NDVI and SR, but there was no improvement regarding the linear models (which are shown in Figure 2).

The relationship between dried biomass and reflectance was also explored using the spectral data gathered with the spectrometrer Fieldspec®3 in Cogollos. Plots 2, 5 and 9 were excluded from the analysis after an exploratory analysis, since they were outliers. The results of the Spearman's rank correlation indicated that only the vegetation indices, NDVI, and SR were correlated to the dried biomass (24 h, 36 h, 48 h) at significance level of 5% ($\alpha = 0.05$). The correlation coefficient between the NDVI and the SR mean, for any of the dried biomass weights was 0.60, while the correlation coefficient between the NDVI and the SR median, for any of the dried biomass weights was 0.55. Therefore the mean values were best correlated with the biomass, and there were no differences for the different dried biomass variables. The stepwise regression conducted with all the variables showed that the best fit model was achieved by using only the SR mean or the NDVI mean values as independent variables. Figure 3 shows the models that were obtained in both of the cases. It should be noted that these results corresponded to dataset B and cannot be compared with the results obtained for dataset A using the Ultracam X image to estimate biomass. The range of the NDVI and the SR values are very different compared to the range of values in dataset A. Figure 3 shows a positive relationship between the vegetation indices and the dried biomass weight. This relationship was expected to be found in the correlations between the dried biomass weight and the spectral indices derived from the Ultracam Xp image from Cogollos (set B). As commented before, the lack of a relationship might be caused by inaccuracies derived from the calibration, positional inaccuracies or the high GSD/plot size ratio.

5. CONCLUSIONS

It was possible to establish a relationship between the radiometric data gathered by the Ultracam and the dried biomass weight in a grassland area. The results were image dependent and it was not possible to find a unique relationship for all of the images from the same set. The vegetation indices (NDVI and SR) were the best predictors for biomass in a grassland area. Nevertheless, more research is needed to test the relationships for other value ranges as well as for other species.

The process to estimate biomass required a previous calibration of the image using the empirical line calibration with portable reflectance targets. The quality of the calibration, as well as the GSD of the image has an impact on the estimation of the dried biomass. More research is needed to assure the quality of the radiometric correction.

There was a relationship between the NDVI and the SR indices derived from the radiometric values that were registered by the spectrometer for each plot, and the dried biomass weight. These relationship should be explored further using the B, G, R and NIR bands defined by the Ultracam filters, to find out the best indices or wavelengths to estimate biomass. This would help to improve the performance of the sensor in this field of research.

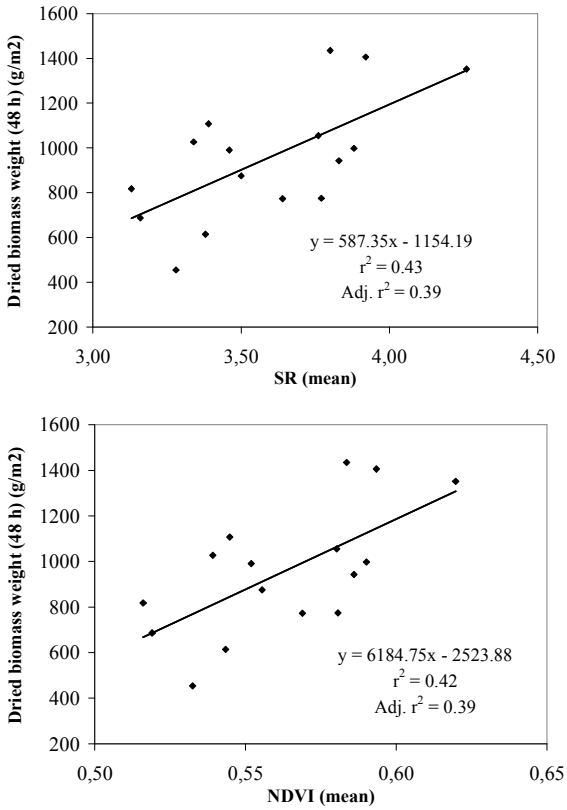

Figure 3. Regression line for dried biomass weight (48 h) and the SR and the NDVI derived from the spectrometer data.

REFERENCES

Alvarez, F., Catanzarite, T., Rodríguez-Pérez, J.R., Nafría, D., 2010. Radiometric calibration and evaluation of Ultracam X and XP using portable reflectance targets and spectrometer data. Application to extract thematic data from imagery gathered by the National Plan of Aerial Orthophotography (PNOA). In: *Proceedings* of the International Calibration and Orientation Workshop *EuroCOW 2010*. 10-12 February 2010, Castelldefels, Spain.

Barrachina, M., Cristóbal, J., Tulla, A., Pons X, 2009. Análisis de la producción de biomasa de los prados y pastos de la Vall Fosca (Pirineo axial-nogueres). In: XIII Congreso de la Asociación Española de Teledetección, Calatayud 23-26 de septiembre de 2009.

Cho, M., Skidmore, A., Corsi, F., van WIEREN, S., SOBHAN, I, 2007. Estimation of green grass/herb biomass from airborne hyoerspectral imagery using spectral indices and partial least squares regression et al. *Int. J. Appl. Earth Observ. Geoinform*. (2007), doi;10.1016/j.jag.2007.2.001

Gao, X., Huete, A.R., Ni, W., Miura, T., 2000. Optical-biophysical relationships of vegetation spectra without background contamination. *Remote Sens. Environ*. 74, pp. 609–620.

Baugh, W. M., Groeneveld, D. P., 2008. Empirical proof of the empirical line. *International Journal of Remote Sensing*, 29 (3), pp. 665–672.

Jensen, J.R., 2005. *Introductory digital image processing: a remote sensing perspective.* Prentice-Hall, New Jersey, pp. 626.

ACKNOWLEDGEMENTS

This research has been partially funded by the Junta de Castilla y León through the project "Calibración radiométrica de cámaras aéreas digitales. Aplicación a la clasificación automática de cubiertas del suelo y estimación de biomasa" (LE001B08).
This research has been developed in collaboration with WIDE WORLD GEOGRAPHIC, S.L. within the project "Calibración radiométrica de imágenes digitales para el control de cambio climático y biomasa en áreas contaminadas o degradadas mediante empleo de la banda infrarroja".
The authors would like to thank Javier Núñez Llamas for all the assistance during the field work and Lucas Martínez for his comments.
The authors would like to thank Bonsai Advanced Technologies for their assistance concerning the use of the spectrometer.